

# Predicting the Drop Performance of Solder Joints by Evaluating the Elastic Strain Energy from High-Speed Ball Pull Tests

TAEHOON YOU,<sup>1</sup> YUNSUNG KIM,<sup>1</sup> JINA KIM,<sup>1</sup> JAEHONG LEE,<sup>2</sup>  
BYUNGWOOK JUNG,<sup>2</sup> JUNGTAH MOON,<sup>2</sup> and HEEMAN CHOE<sup>1,3</sup>

1.—School of Advanced Materials Engineering, Kookmin University, Chungneung-dong, Songbuk-ku, Seoul 136-702, South Korea, 2.—MK Electron Co., Ltd., 316-2 Geumeoh-ri, Pogok-eup, Cheoin-gu, Yongin-si, Gyeonggi Province 449-812, South Korea. 3.—e-mail: heeman@kookmin.ac.kr

Despite being expensive and time consuming, board-level drop testing has been widely used to assess the drop or impact resistance of the solder joints in handheld microelectronic devices, such as cellphones and personal digital assistants (PDAs). In this study, a new test method, which is much simpler and quicker, is proposed. The method involves evaluating the elastic strain energy and relating it to the impact resistance of the solder joint by considering the Young's modulus of the bulk solder and the fracture stress of the solder joint during a ball pull test at high strain rates. The results show that solder joints can be ranked in order of descending elastic strain energy as follows: Sn-37Pb, Sn-1Ag-0.5Cu, Sn-3Ag-0.5Cu, and Sn-4Ag-0.5Cu. This order is consistent with the actual drop performances of the samples.

**Key words:** Solder joint, SnAgCu, deformation and fracture, intermetallic alloys and compounds, mechanical properties, elastic properties

## INTRODUCTION

Lead-free solders, particularly Sn-Ag-Cu, are becoming increasingly popular in the electronic packaging industry, due to the environmental concerns associated with lead.<sup>1-6</sup> Sn-Ag-Cu solders possess several advantages over conventional Sn-Pb solders. These include higher stiffness and strength, and superior resistance to thermal cycling and fatigue as well as their high microstructural stability.<sup>2,7,8</sup> However, the fact that they are stiffer and more brittle also makes them more prone to brittle failure during impact loading, which is frequently encountered in microelectronic packages for handheld electronic devices.<sup>1,9</sup> A number of different methodologies (e.g., drop impact, high-speed ball shear or ball pull, and tensile bond tests) to simulate and understand the fracture behavior of a solder joint under high-strain-rate loads have been attempted.<sup>5,10</sup> However, among the various existing

test methodologies, only the board-level drop test, proposed by the Joint Electron Device Engineering Council (JEDEC), has been widely acknowledged for providing a common test reference for the industry in assessing the drop performance of microelectronic solder joints. Nevertheless, the JEDEC's standard board-level drop test method is generally too costly and time consuming to be viable.<sup>10,11</sup> Furthermore, the data obtained from this technique make it rather difficult to determine the inherent resistance of the solder joint to impact loadings. This is because it is almost impossible to distinguish between the impact responses of the solder material, the board, and any other packaging materials.

In this article, we propose a new method of quantitatively evaluating the impact resistance of a solder joint. The method involves the analysis of the solder joint's elastic strain energy during high-speed tensile loading. The solder material's Young's modulus and the fracture stress of the intermetallic-compound (IMC) interfaces under the high-speed pull test conditions are the only measurements required.

(Received August 12, 2008; accepted December 4, 2008;  
published online January 10, 2009)

## MATERIALS AND EXPERIMENTAL PROCEDURE

Four different types of commercially available ball grid array (BGA) solder balls (MK Electron, Korea) were examined in this study. Their compositions were as follows: Sn-1Ag-0.5Cu, Sn-3Ag-0.5Cu, Sn-4Ag-0.5Cu, and eutectic Sn-37Pb. They are hereafter denoted as SAC 105, SAC 305, SAC 405, and Sn-Pb, respectively. Each BGA solder ball used in this study had a diameter of 400  $\mu\text{m}$ . Electroless nickel immersion gold (ENIG) was used for the solder pad finish. The solder balls were attached to the substrates in a seven-zone convective reflow oven (1706 EXL, Heller) containing a nitrogen atmosphere. All of the samples were reflowed twice. The soldering profile had a  $150 \pm 2^\circ\text{C}$  preheat temperature, with a peak temperature of  $\sim 245^\circ\text{C}$ .

The high-speed pull tests were performed using Dage 4000HS bond tester at a speed of 400 mm/s. Each set of pull test data consists of at least 15 measurements.

The Young's moduli were determined by an ultrasonic wave reflection measurement technique using rectangular parallelepiped specimens with dimensions of 3 cm  $\times$  3 cm  $\times$  2 cm. The longitudinal and transverse speeds of sound through the specimens were measured using 50 MHz transducers connected to a digital oscilloscope. The Poisson's ratio and Young's modulus of each sample were then calculated according to Ref. 12.

## RESULTS AND DISCUSSION

### Measurement of Young's Modulus

The Young's modulus of a metallic material is usually measured by a loading-unloading measurement technique in tension. However, the linear elastic portion of the tensile stress-strain curve in most Sn-rich alloys is limited, which makes accurate measurement of the Young's modulus quite difficult.<sup>3</sup> Therefore, in this study, the Young's moduli were measured by the previously mentioned ultrasonic measurement method, the results of which are displayed in Table I. Young's moduli values from

the literature are also shown for comparison. The Young's moduli of Sn-Pb, SAC 105, SAC 305, and SAC 405 were found to be 34 GPa, 43 GPa, 48 GPa, and 52 GPa, respectively. The higher moduli of SAC 305 and SAC 405 compared with that of SAC 105 can be attributed to the higher amounts of the  $\text{Ag}_3\text{Sn}$  phase formed in the bulk solders of SAC 305 and SAC 405.<sup>7,16,17</sup>

### High-Speed Ball Pull Test

The failure mode distributions for the high-speed ball pull tests of the Sn-Pb, SAC 105, SAC 305, and SAC 405 solder joints are shown in Fig. 1a. It is well known that increasing the test speed increases the likelihood of brittle failure.<sup>5,9</sup> This explains why the samples in this study, which were tested at the high speed of 400 mm/s, underwent primarily brittle failure, as shown in Fig. 2. In fact, all of the Sn-Ag-Cu samples underwent brittle failure. By comparison, only 28% of the eutectic Sn-Pb solder joints underwent brittle failure (the remaining 72% experienced ductile failure). These results are consistent with those from other high-strain-rate tests.<sup>9,18</sup> The fact that the Sn-Pb solder joints undergo ductile failure more frequently is in good agreement with the report that the strength and stiffness of the Sn-Pb solders are generally lower than those of the Sn-Ag-Cu solders.<sup>2</sup>

The average fracture stresses for the three types of Sn-Ag-Cu solder joints during the high-speed pull tests are presented in Fig. 1b. The results for the eutectic Sn-Pb samples are also shown for comparison. In this study, the fracture stress was calculated by dividing the average pull force by the estimated contact area between the solder ball and the pad. All of the Sn-Ag-Cu alloy solders showed similar fracture stresses (when taking the error ranges into consideration). The eutectic Sn-Pb solders showed a higher fracture stress. The reason for these results is thought to be as follows. The primary IMC layer that forms in the eutectic Sn-Pb solder joint is  $\text{Ni}_3\text{Sn}_4$ . This is known to be thinner and hence stronger than the  $(\text{Cu},\text{Ni})_6\text{Sn}_5$  layer that is formed in all of the Sn-Ag-Cu solder joints. The structures of the  $(\text{Cu},\text{Ni})_6\text{Sn}_5$  IMC interfaces in the Sn-Ag-Cu alloys are similar for all three samples, regardless of their different Ag contents.<sup>7</sup>

### Evaluating the Impact Resistance of a Solder Joint

At high strain rates between  $10^3/\text{s}$  and  $10^5/\text{s}$ , the material experiences impact conditions and may fail with reduced fracture energy in a brittle manner. This phenomenon can be well described by the relationship between the true stress and the strain rate, which shows that the strength increases but the plastic deformation decreases with increasing strain rate as follows<sup>19</sup>:

$$\sigma = K\dot{\epsilon}^m, \quad (1)$$

Table I. Young's Moduli of the Sn-Based Solder Alloys

Alloy	Young's Modulus (GPa, Present Study)	Young's Modulus (GPa, Other Studies)
Sn-Pb	<sup>a</sup> 34	<sup>b</sup> 38, <sup>13</sup> <sup>c</sup> 35, <sup>14</sup> <sup>c</sup> 20 <sup>15</sup>
Sn-1Ag-0.5Cu	<sup>a</sup> 43	<sup>a</sup> 47, <sup>7,16</sup>
Sn-3Ag-0.5Cu	<sup>a</sup> 48	<sup>a</sup> 51, <sup>7,16</sup>
Sn-4Ag-0.5Cu	<sup>a</sup> 52	<sup>c</sup> 40 <sup>15</sup> , <sup>a</sup> 53 <sup>7,16</sup>

From <sup>a</sup>ultrasonic measurement, <sup>b</sup>single-crystal elasticity theory, and <sup>c</sup>tensile test.

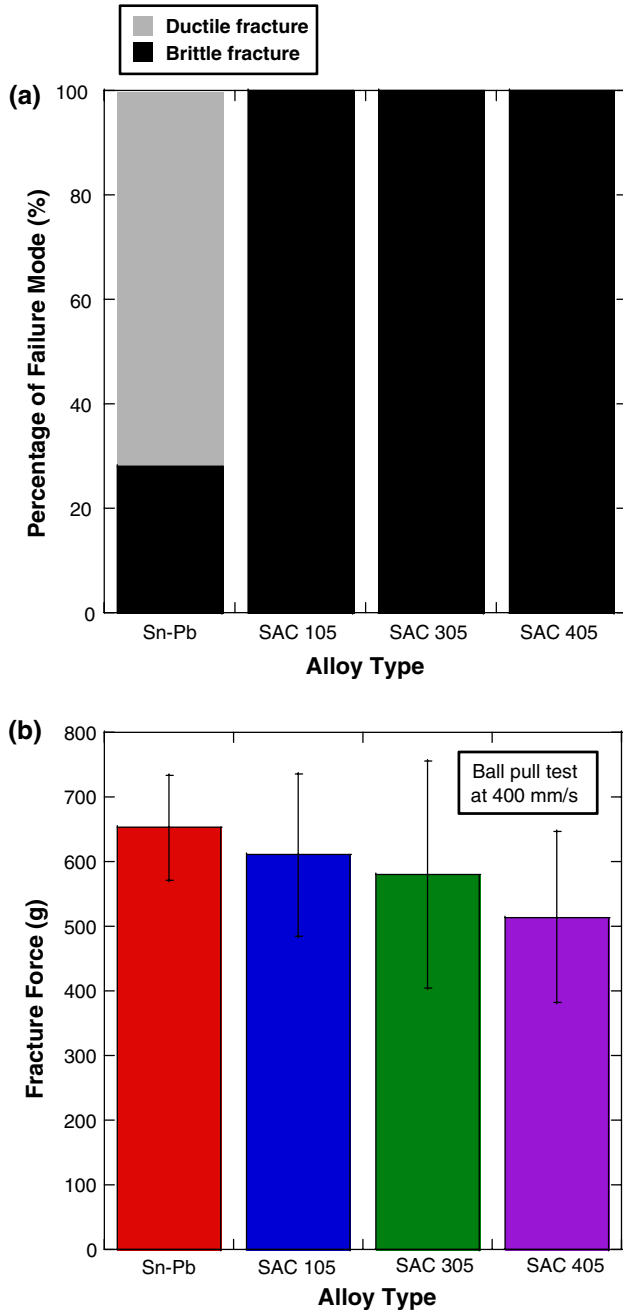


Fig. 1. (a) Failure mode distributions for the high-speed ball pull tests at 400 mm/s with the ENIG surface finish. (b) The high-speed ball pull fracture forces for the different samples tested under the same conditions.

where  $m$  is the strain-rate sensitivity factor,  $\dot{\epsilon}$  is the strain rate,  $K$  is the material constant, and  $\sigma$  is the true stress.

Here, based on the assumption that there is no or insignificant plastic deformation during the impact event at very high strain rates,<sup>5,20</sup> we are quantitatively estimating the impact resistance of a solder joint, i.e., a solder ball plus the IMC interfaces formed by the specific combination of solder ball and pad surface finish. The instantaneously stored

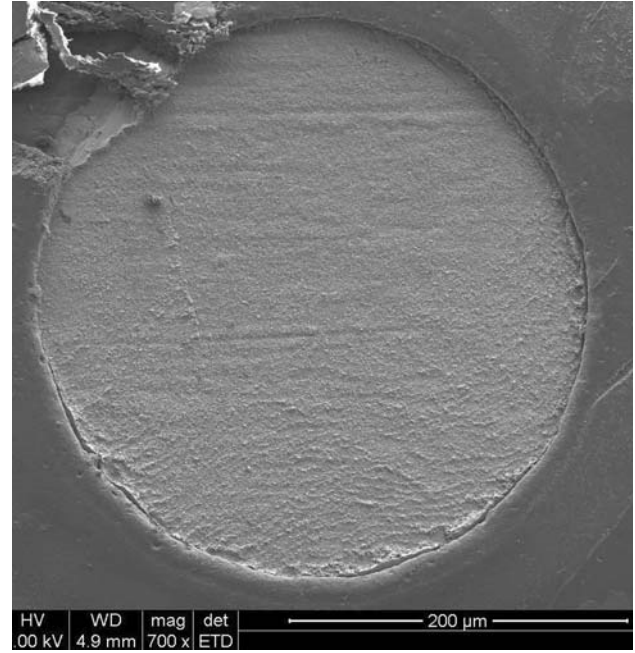


Fig. 2. Typical brittle fracture surface of Sn-1%Ag-0.5%Cu after the high-speed ball pull test at 400 mm/s.

elastic strain energy of the solder joint per unit volume should then be representative of the impact tolerance of the solder joint. The strain energy per unit volume or strain energy density ( $U_o$ ) of a material during tension loading is generally represented as follows<sup>21</sup>:

$$U_o = \frac{1}{2} \cdot \sigma_f \cdot \epsilon_f = \frac{\sigma_f^2}{2E}, \quad (2)$$

where  $\sigma_f$  and  $\epsilon_f$  are, respectively, the final stress and strain for the elastic deformation, and  $E$  is the Young's modulus of the material.

Therefore, the total strain energy of a solder joint (a solder ball plus the IMC layers) at the fracture event during impact loading is the sum of the elastic energy stored in the solder ball and the elastic energy stored in the IMC interfaces, as shown schematically in Fig. 3. However, the elastic energy for the IMC interfaces can simply be ignored, because their average Young's modulus is very high (the Young's modulus of  $\text{Ni}_3\text{Sn}_4$  is 130 GPa to 150 GPa,<sup>22</sup> and that of  $(\text{Cu,Ni})_6\text{Sn}_5$  is 150 GPa to 210 GPa<sup>22</sup>) compared with that of the bulk solder ball ( $\sim 34$  GPa to 52 GPa, Table I). Moreover, their estimated volume is significantly small compared with that of the solder ball ( $\sim 400$  μm diameter); the ratio of their volumes is approximately 1:350, assuming that the thickness of the IMC interfaces is about 1 μm to 2 μm.<sup>7</sup> The total elastic energy is then roughly the elastic energy instantaneously stored in the solder ball until the impact fracture occurs. In other words, the total elastic strain energy,  $U_{\text{total}}$ , is then given by

**Table II. Calculation of the Elastic Strain Energy at Impact Fracture Under a High-Speed Ball Pull Test Using Eqs. 2 and 3**

Alloy	Estimated Volume (m <sup>3</sup> )	Fracture Stress (MPa)	Strain Energy Density, U <sub>o</sub> (J/m <sup>3</sup> )	Elastic Strain Energy, U <sub>o</sub> × Vol. (μJ)
Sn-Pb	~3.3 × 10 <sup>-11</sup>	51.0	38176	1.28
SAC 105	~3.3 × 10 <sup>-11</sup>	47.7	26428	0.89
SAC 305	~3.3 × 10 <sup>-11</sup>	45.3	21333	0.71
SAC 405	~3.3 × 10 <sup>-11</sup>	40.1	15466	0.52

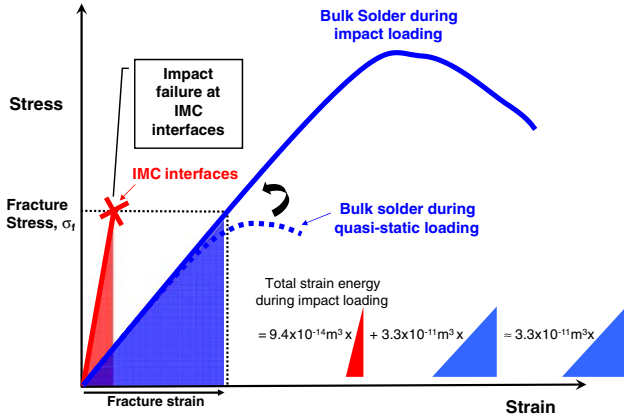


Fig. 3. Schematic of the stress–strain behavior of IMC interfaces and bulk solder during tensile loading at high-strain rates. It should be noted that the total strain energy during the impact loading is the area under the curve multiplied by the volume of the solder joint.

$$\begin{aligned}
 U_{\text{total}} &= U_o^{\text{IMC}} \times \text{Vol.}^{\text{IMC}} + U_o^{\text{solder}} \times \text{Vol.}^{\text{solder}} \\
 &\approx U_o^{\text{solder}} \times \text{Vol.}^{\text{solder}} = \frac{\sigma_f^2}{2E} \times \text{Vol.}^{\text{solder}}, \quad (3)
 \end{aligned}$$

where  $U_o^{\text{IMC}}$  and  $U_o^{\text{solder}}$  are the strain energies per unit volume, and  $\text{Vol.}^{\text{IMC}}$  and  $\text{Vol.}^{\text{solder}}$  are the estimated volumes of the IMC layers and the bulk solder, respectively,  $\sigma_f$  is the stress when the impact fracture takes place, and  $E$  is the Young’s modulus of the bulk solder. In this investigation,  $\sigma_f$  represents the fracture stress obtained during the high-speed ball pull test at 400 mm/s for each type of solder joint, as shown in Fig. 1b.

The total elastic strain energy,  $U_{\text{total}}$ , is calculated using Eq. 3 and is displayed in Table II. The materials ranked in descending order of resistance to impact loading are Sn-Pb, SAC 105, SAC 305, and SAC 405. This order of impact resistance is in good agreement with the order of the actual drop performances of the same solder joints reported in the literature; Sn-Pb solder joints are reported to be superior in drop performance to Sn-Ag-Cu solder joints (for identical ENIG surface finishes).<sup>1,9</sup> Furthermore, the drop performance of SAC 105 is known to be greater than that of SAC 305 or SAC 405.<sup>8,16</sup> There can be two reasons why Sn-Pb solder joints are superior to Sn-Ag-Cu solder joints

in terms of resistance to impact loading. Firstly, the Sn-Pb bulk solder is more compliant than the Sn-Ag-Cu bulk solder, as displayed in Table I. Secondly, the Ni<sub>3</sub>Sn<sub>4</sub> IMC layer is generally known to be thinner and hence more robust than the (Cu,Ni)<sub>6</sub>Sn<sub>5</sub> layer.<sup>7</sup> On the other hand, the higher resistance to impact loads of the lower-silver-content Sn-Ag-Cu solder joints may be attributed to their bulk properties, but little to their IMC interfaces.<sup>7</sup>

The method introduced in this study can be utilized to quantitatively estimate the impact resistance and hence drop performance of a solder joint by simply combining the Young’s modulus of the bulk solder and the fracture stress measured from a high-speed ball pull test. This technique is simple to perform, regardless of the size of the solder sphere or the type of surface finish used. This means that a quick evaluation of the impact resistance of a solder joint, based solely on the properties of the solder joint material, is possible. It is also noted that the aforementioned testing method is, however, unproven with respect to evaluating solder joints with different BGA designs and layouts, which might also have effects on the drop performance in the JEDEC and other test methods. In addition, the discussed test method may have limitations in correctly simulating the field conditions when more complex stress states, such as bending and cyclic stress, are involved where an unusual crack propagation behavior is typically identified.<sup>23</sup>

## CONCLUSIONS

A new method has been introduced to predict the drop performance of a solder joint to potentially replace the costly and complicated board-level drop test. This new method is based on the strain energy concept during impact loadings and simply requires the Young’s modulus of the solder material and the fracture stress under a high-speed ball pull test to be measured. The obtained results are in excellent agreement with literature reports.

## ACKNOWLEDGEMENTS

This research was supported by Seoul R&BD Program (Grant No. NT070083). HC also acknowledges partial support from the 2008 research fund of Kookmin University in the Republic of Korea.



## REFERENCES

1. Y.S. Lai, P.F. Yang, and C.L. Yeh, *Microelectron. Reliab.* 46, 645 (2006). doi:[10.1016/j.microrel.2005.07.005](https://doi.org/10.1016/j.microrel.2005.07.005).
2. M. Abtew and G. Selvaduray, *Mater. Sci. Eng. Rep.* 27, 95 (2000). doi:[10.1016/S0927-796X\(00\)00010-3](https://doi.org/10.1016/S0927-796X(00)00010-3).
3. N. Chawla and R.S. Sidhu, *J. Mater. Sci. Mater. Electron.* 18, 175 (2007). doi:[10.1007/s10854-006-9028-0](https://doi.org/10.1007/s10854-006-9028-0).
4. X. Deng, M. Koopman, N. Chawla, and K.K. Chawla, *Mater. Sci. Eng. A* 364, 240 (2004). doi:[10.1016/j.msea.2003.08.032](https://doi.org/10.1016/j.msea.2003.08.032).
5. Y.S. Lai, H.C. Chang, and C.L. Yeh, *Microelectron. Reliab.* 47, 2179 (2007). doi:[10.1016/j.microrel.2006.11.015](https://doi.org/10.1016/j.microrel.2006.11.015).
6. Y. Xia and X. Xie, *J. Alloy. Comp.* 457, 198 (2008). doi:[10.1016/j.jallcom.2007.03.038](https://doi.org/10.1016/j.jallcom.2007.03.038).
7. Y.T. Chin, P.K. Lam, H.K. Yow, and T.Y. Tou, *Microelectron. Reliab.* 48, 1079 (2008). doi:[10.1016/j.microrel.2008.04.003](https://doi.org/10.1016/j.microrel.2008.04.003).
8. M. Amagai, Y. Toyoda, and T. Tajima, *Proc. 53rd Electron. Comp. Tech. Conf.* (New Orleans, LA: IEEE, 2003), p. 317.
9. F. Song, S.W.R. Lee, K. Newman, B. Sykes, and S. Clark, *Proc. 57th Electron. Comp. Tech. Conf.* (Reno, NV: IEEE, 2007), p. 364.
10. S.-J. Jeon, S. Hyun, H.-J. Lee, J.-W. Kim, S.-S. Ha, J.-W. Yoon, S.-B. Jung, and H.-J. Lee, *Microelectron. Eng.* 85, 1967 (2008).
11. E.H. Wong, R. Rajoo, S.K.W. Seah, C.S. Selvanayagam, W.D. van Driel, J.F.J.M. Caers, X.J. Zhao, N. Owens, L.C. Tan, M. Leoni, P.L. Eu, Y.-S. Lai, and C.-L. Yeh, *Microelectron. Reliab.* 48, 1069 (2008). doi:[10.1016/j.microrel.2008.04.008](https://doi.org/10.1016/j.microrel.2008.04.008).
12. P. Majumdar, S.B. Singh, and M. Chakraborty, *Mater. Sci. Eng. A* 489, 419 (2008). doi:[10.1016/j.msea.2007.12.029](https://doi.org/10.1016/j.msea.2007.12.029).
13. C. Basaran and J. Jiang, *Mech. Mater.* 34, 349 (2002). doi:[10.1016/S0167-6636\(02\)00131-X](https://doi.org/10.1016/S0167-6636(02)00131-X).
14. R.J. McCabe and M.E. Fine, *Scr. Mater.* 39, 189 (1998). doi:[10.1016/S1359-6462\(98\)00149-3](https://doi.org/10.1016/S1359-6462(98)00149-3).
15. C. Andersson, P. Sun, and J. Liu, *J. Alloy. Comp.* 457, 97 (2008). doi:[10.1016/j.jallcom.2007.03.028](https://doi.org/10.1016/j.jallcom.2007.03.028).
16. D. Suh, D.W. Kim, P. Liu, H. Kim, J.A. Weninger, C.M. Kumar, A. Prasad, B.W. Grimsley, and H.B. Tejada, *Mater. Sci. Eng. A* 460–461, 595 (2007). doi:[10.1016/j.msea.2007.01.145](https://doi.org/10.1016/j.msea.2007.01.145).
17. K. Zeng and K.N. Tu, *Mater. Sci. Eng. Rep.* 38, 55 (2002). doi:[10.1016/S0927-796X\(02\)00007-4](https://doi.org/10.1016/S0927-796X(02)00007-4).
18. M. Arra, D. Xie, and D. Shangquan, *Proc. 52nd Electron. Comp. Tech. Conf.* (San Diego, CA: IEEE, 2002), p. 1256.
19. R.W. Hertzberg, *Deformation and Fracture Mechanics of Engineering Materials*, 4th ed. (New York: Wiley, 1995).
20. Y. Zhao, C. Basaran, C. Cartwright, and T. Dishongh, *Mech. Mater.* 32, 161 (2000). doi:[10.1016/S0167-6636\(99\)00053-8](https://doi.org/10.1016/S0167-6636(99)00053-8).
21. J. Beddoes and M.J. Bibby, *Principles of Metal Manufacturing Processes* (London: Arnold, 1999).
22. L. Xu and J.H.L. Pang, *Thin Solid Films* 504, 362 (2006). doi:[10.1016/j.tsf.2005.09.056](https://doi.org/10.1016/j.tsf.2005.09.056).
23. J. Caers, X. Zhao, E.H. Wong, S. Seah, C.S. Selvanayagam, W.D. van Driel, N. Owens, M. Leoni, L.C. Tan, P.L. Eu, Y.-S. Lai, and C.-L. Yeh, *58th Electronic Components and Technology Conference* (Lake Buena Vista, FL: ECTC, 2008).